Available online at www.sciencedirect.com
ScienceDirect
Vibrational Spectroscopy 41 (2006) 176–181
VIBRATIONAL SPECTROSCOPY
www.elsevier.com/locate/vibspec

In situ adsorption densities of polyacrylates on hematite nano-particle films as determined by ATR-FTIR spectroscopy

Wilhelm van Bronswijk [a,*], Luke J. Kirwan [a,1], Phillip D. Fawell [b]

[a] *Parker Cooperative Research Centre for Integrated Hydrometallurgy Solutions, Department of Applied Chemistry, Curtin University of Technology, GPO Box U1987, Perth, WA 6845, Australia*
[b] *Parker Cooperative Research Centre for Integrated Hydrometallurgy Solutions, CSIRO Minerals, PO Box 90, Bentley, WA 6982, Australia*

Received 3 November 2005; received in revised form 12 December 2005; accepted 19 December 2005
Available online 17 February 2006

Abstract

The adsorption of polymers is typically characterised by segments of adsorbed ''trains'' and unadsorbed ''loops'' and ''tails''. Attenuated total reflectance infrared spectroscopy is thus an ideal means of studying this process in situ. In this study the adsorption of long chain polyacrylates onto hematite at pH 2 and 13 has been examined using a single bounce Horizontal-ATR cell. The crucial parameters that affect surface adsorbed densities obtained by this method are the depth of penetration and effective path length of the evanescent wave, and the infrared absorbtivities of the free and bound polyacrylate. The former require a detailed knowledge of the optical properties of the interface (refractive indices, incidence angles and polarisation fraction) whilst the latter can only be approximated, as it is not possible to measure the infrared absorptivity, nor the refractive index, of adsorbed polyacrylate independently. The results obtained show that only ~2–10% of the polymer chain is adsorbed, thereby confirming the ''loops, tails and trains'' mode of adsorption, and that higher molecular weight polyacrylates adsorb with a lower fraction of adsorbed segments.

Keywords: Polyacrylates; Hematite; Adsorption; Surface density; Attenuated total reflectance fourier transform infrared

1. Introduction

The Bayer process for the extraction of alumina from bauxite generates large volumes of solid waste which generally consists of iron oxides and oxyhydroxides (hematite and goethite), silica and aluminosilicates (de-silication products), which is usually referred to as ''red mud''. This residue has a small particle size and is flocculated to improve settling and hence solid–liquid separation. Polyacrylates and acrylate/acrylamide co-polymers are often used for this purpose [1].

In almost all mineral systems, flocculant adsorption proceeds through hydrogen bonding of amide functionalities to neutral oxide groups on the substrate surface. This is not possible for polyacrylate flocculants in Bayer liquor (high pH, high ionic strength), for which the adsorption process is poorly understood. In view of the complex nature of the Bayer residues, mechanistic studies have focused on model substrates such as hematite. Whilst ex situ and in situ studies contrasting the adsorption mechanisms for polyacrylates on hematite under low and high pH conditions have been reported [2–4] adsorption densities have only been reported from ex situ studies [2].

Adsorption density studies are often based on solution depletion and/or adsorbate recovery procedures [5,6] and as such do not take into account the free and bound segments of the adsorbed polymer arising from its loop, tail and train configuration [7]. Attenuated total reflectance fourier transform infrared (ATR-FTIR) spectroscopy is a much more promising technique in this regard, as it often enables free and bound functional groups to be differentiated on the basis of changes to their vibrational frequencies [3,4]. For these types of studies the ATR element must first be coated with a thin layer of the substrate, with the method relying on the evanescent wave penetrating the substrate film and interacting with the adsorbed substrate and solution.

ATR-FTIR spectroscopy follows Beer's law ($A = \varepsilon c d_e$), where infrared absorptivity (ε, m mol^{-1} or m g^{-1}) of the

* Corresponding author. Tel.: +61 8 9266 7321; fax: +61 8 9266 2300.
E-mail address: w.vanbronswijk@curtin.edu.au (W. van Bronswijk).
[1] Present address: Aughinish Alumina Ltd., Askeaton, Co. Limerick, Ireland.

0924-2031/$ – see front matter
doi:10.1016/j.vibspec.2005.12.007

species, its concentration (c, g m^{-3}), cell path length or effective thickness (d_e, m), and integrated band absorbance (A, m^{-1}) are expressed in SI base units. This equation is applicable only when solutes are evenly distributed in a phase. When a species is directly adsorbed onto an ATR plate it becomes a two-layer problem (the adsorbed layer and the solution beyond) provided that the refractive indices of the adsorbate and solution are less than that of the ATR plate and total internal reflection occurs. Absorbance is then described by the equation first proposed by Sperline et al. [8],

$$A = \frac{\Gamma \varepsilon d_e}{d_p} + \varepsilon c_b d_e$$

where Γ is the surface density (g m^{-2}) of the adsorbed species, d_p the depth of penetration and c_b is the solution concentration.

Sperline et al. [9] also proposed an equation for a three-layer system of substrate film, adsorbed species and the solution beyond,

$$A = \frac{\Gamma \varepsilon d_{e,3}}{d_3} + \varepsilon c_b d_{e,3}$$

where $d_{e,3}$ and d_3 are the effective path length and depth of penetration in the third layer.

The first term in both equations expresses the absorbance of the adsorbed species in terms of an equivalent solution concentration and thickness or depth of penetration (d_p), whilst the second term simply accounts for the contribution of unadsorbed solution species to the measured absorbance. Attenuation by the film is taken into account in the three-layer system and requires the time-average square of the electric fields in those layers to be calculated [10], but ignored in the two-layer system, where it is assumed that the absorbed layer has negligible thickness [8]. This assumption is reasonable for small molecules such a surfactants, but may not be for high molecular weight polymers.

Thus surface densities obtained from ATR absorbance measurement will be influenced greatly by the optical properties of the ATR element, substrate film, adsorbed species and solution that govern the effective path lengths and depths of penetration. A further complication arises when a flat plate ATR element is used, as the effective path length for incident radiation parallel and perpendicular to the plate are not the same. An accurate assessment of the refractive indices of the ATR element, substrate film, adsorbate and solution, and the polarisation of the infrared radiation, are thus essential to obtaining meaningful adsorption density data.

2. Experimental

2.1. Polyacrylate solutions

Concentrated stock solutions of polyacrylates (Aldrich, polyacrylic acid of average molecular weight ~2000 and ~4.5×10^5, referred to as PAA2K and PAA450K respectively, and Ciba Specialty Chemicals sodium polyacrylate of average molecular weight ~1.3×10^7, referred to as PAA13M) were prepared by the addition of the powdered polymer to the appropriate aqueous solution and steady stirring for several days. Dilutions were made from the stock solutions as required.

2.2. Hematite nano-particle preparation and deposition

The hematite colloid was prepared from $FeCl_3$ and HCl, and characterised, as previously described [3]. A thin layer of particles was formed on the ZnSe ATR crystal by dispensing 30 μL of colloid to a diameter of 5 mm and allowing it to dry. Absorbances measurements of water droplets of various sizes showed that the measurement area of the cell was ~3 mm diameter and atomic force microscopy measurements of the film showed it to have a uniform thickness of ~900 nm, apart from an edge ridge of <0.2 mm width.

2.3. FTIR-ATR measurements

Spectra were recorded as reported previously [3] at 4 cm^{-1} resolution on a Bruker IFS66 spectrometer fitted with a flow through Harrick ''Seagull'' single bounce variable angle ATR accessory and MCT detector, with 256 scans being accumulated. The cell was brought to equilibrium with a solution of the required pH before being contacted with polyacrylate solutions, at a flow rate of 1 mL min^{-1}. At high pH, the solutions also consisted of a background electrolyte (1.0 M NaCl), as it was previously established that the polymers require the presence of a cationic species at a suitable concentration to facilitate adsorption [4]. The background used for all spectra was that of the clean dry ZnSe crystal. A number of backgrounds were recorded to simplify the removal of water vapour and carbon dioxide peaks. Peak areas were determined from horizontal baselines for water and benzene, and valley–valley baselines for solution and adsorbed polyacrylates, using Bruker Optus V2.0 software.

3. Results and discussion

3.1. Characterisation of the ATR solid–liquid interface

The crucial parameters for determining adsorption densities are the depth of penetration of the evanescent wave and effective thickness (path length) of the sample. These are critically dependent on the refractive indices of the ATR/film/adsorbate/solution interface. Determining these experimentally with a Horizontal ATR (flat plate HATR) requires that the degree of polarisation of the radiation and its incident angle be known accurately.

3.2. Polarisation ratio

As a first step in determining the polarisation ratio, the integrated molar absorptivity of water was obtained with a fixed path length transmission cell for the weakly absorbing region from 2000 to 2250 cm^{-1} and found to be 1554 m mol^{-1}. This in turn enabled the effective path length (d_e) for the ATR accessory to be experimentally determined ($d_e = A/\varepsilon c$). For HATR spectroscopy the effective thickness

(d_e) has components from both parallel and perpendicular polarised radiation [11], i.e.

$$d_e = Xd_{e||} + (1 - X)d_{e\perp}$$

$$d_{e||} = \frac{n_{21}\lambda(2\sin^2\theta - n_{21}^2)\cos\theta}{n_1\pi(1 - n_{21}^2)[(1 + n_{21}^2)\sin^2\theta - n_{21}^2](\sin^2\theta - n_{21}^2)^{1/2}}$$

$$d_{e\perp} = \frac{n_{21}\lambda\cos\theta}{n_1\pi(1 - n_{21}^2)(\sin^2\theta - n_{21}^2)^{1/2}}$$

and d_e and d_p are related by

$$d_e = \frac{n_{21}\cos\theta}{1 - n_{21}^2}\left[1 + \frac{2\sin^2\theta - n_{21}^2}{(1 - n_{21}^2)\sin^2\theta - n_{21}^2}\right]d_p$$

where X is the fraction of parallel polarised radiation, $n_1 = 2.430$ (ZnSe – 2125 cm^{-1}) [12], $n_2 = 1.320$ (water – 2125 cm^{-1}) [13], $n_{21} = n_2/n_1$, θ the incident angle and λ is the wavelength of the radiation.

X can then be obtained from the experimental value of d_e and the known values of n_1, n_2, θ and λ by assuming a trial value for X, calculating X from the above equations and iteratively minimising $\Sigma[d_{e(expt)} - d_{e(calc)}]^2$.

Table 1 shows that for the instrumentation used, the ratio of infrared polarisation remains fairly consistent with approximately 39% parallel and 61% perpendicular polarisation at the incident angles of 45° and 50°, and that d_e and d_p vary with θ as expected.

3.3. Refractive indices

Once the polarisation fractions of the system have been established it is a simple task to determine the refractive index of one medium if that of the other medium is known, from absorbances measured at two incident angles, since ε and c will be constants, e.g.

$$\frac{A_{45}}{A_{50}} = \frac{d_{e45}}{d_{e50}} = \frac{0.387d_{e||} + 0.613d_{e\perp}}{0.392d_{e||} + 0.608d_{e\perp}}$$

Knowing the values of X, n_1, θ, λ, and assuming a trial value for n_2 allows a value of A_{45}/A_{50} to be calculated and $[(A_{45}/A_{50(expt)}) - (A_{45}/A_{50(calc)})]^2$ can be minimised iteratively to obtain the best fit value of n_2. The result obtained for benzene at 2210 cm^{-1}, $n_2 = 1.52$, is in reasonable agreement with the previously reported value of 1.48 [14] and within the experimental error of the procedure used.

ATR-FTIR determinations of refractive index are usually carried using a circular rod ATR element, rather than a flat plate, as this scrambles the polarisation and X ceases to be an issue. This allows incident angles to be accurately determined for these cells. Independent characterisation of X is not possible for HATR without knowing an accurate incident angle, and vice versa. The higher value obtained for the refractive index of benzene is most likely due to inaccuracies in the incident angle, which have a more significant effect on the refractive index determination than variations in the X value.

Despite the uncertainties associated with determining refractive indices by HATR, it can still be utilised as a tool for determining adsorption densities, as the crucial parameter is d_e/d_p and both d_e and d_p are similarly affected by n and θ.

Table 1
Observed absorbance of water, fraction of parallel (X) infrared radiation, effective path length and depth of penetration at 45° and 50° incident angles (ZnSe/H_2O, 2125 cm^{-1})

Incident angle, θ	Abs. (m^{-1})	X	d_e (nm)	d_p (nm)
45°	88.9	0.387	1029	681
50°	65.8	0.392	762	571

3.4. Hematite coated optics

The hematite coated optics present an interesting problem, as the refractive index of hematite (2.91) is greater than that of both ZnSe (2.43) and water (1.32). If the hematite was a solid film there would be refraction in going from ZnSe to hematite, internal reflection at the hematite water interface and again in going from hematite to ZnSe, effectively trapping the radiation in the hematite film. However, in this study the films used consist of nano-particles (diameter ~50 − 150 nm), are porous and contain solvent. If the refractive indices of the porous films were intermediate between water and ZnSe then conventional ATR behaviour would occur. That appears to be the case as adsorbate spectra are readily observed (Fig. 1) [3,4], and suggests that the system is best treated as a two-layer problem, i.e. adsorption to a reactive ATR element, with the radiation passing both ways through the hematite layer and the hematite coated ZnSe acting optically as a single entity.

To assess this, the refractive index of hematite coated ZnSe was determined at 2125 cm^{-1} using water ($n = 1.320$) as the contacting liquid and measuring its absorbance at 45° and 50°. The value obtained was 2.319, which is slightly less than ZnSe (2.43) and significantly less than hematite (2.91). If it is assumed that the pores of the hematite are filled with water a refractive index of 2.319 is the weighted average of 67% hematite and 33% water. This is close to the 26% void fraction found for mono-sized close packed spheres [15], which

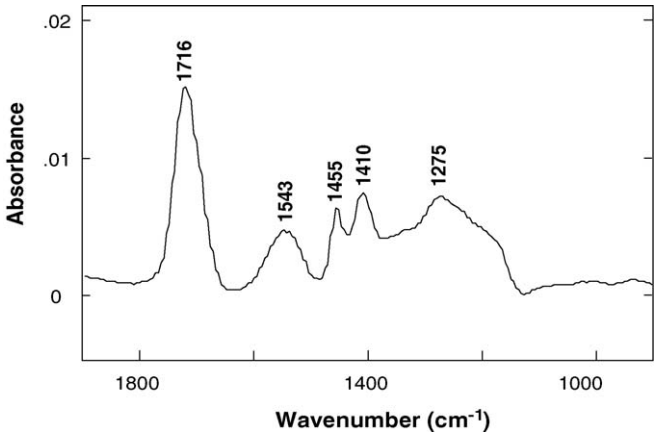

Fig. 1. Spectrum, after water subtraction, of PAA450K adsorbed on hematite from a 50 ppm solution at pH 2.

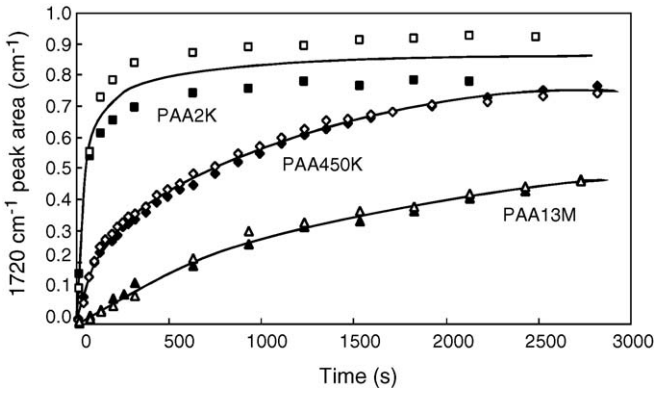

Fig. 2. Adsorption of polyacrylic acid at pH 2 as monitored by the area of the carbonyl stretching peak (1720 cm^{-1}) as a function of time and polymer molecular weight.

suggests that a porous film with approximately 33% water is a reasonable model, particularly considering that the hematite film is not made up exclusively of uniform spherical particles. It can therefore be concluded that a two-layer model appropriately describes the solid–liquid interface for a hematite nano-particle film cast onto a ZnSe HATR element.

The cast hematite films have a high degree of reproducibility, as shown by adsorption from 50 ppm PAA2K, PAA450K and PAA13M solutions onto fresh films as a function of time (Fig. 2). With the exception of PAA2K, where the short chains probably penetrate the hematite films to different degrees depending on particle packing, the polymers appear to adsorb only to the outer layer of particles, thereby giving reproducible surfaces and adsorption.

3.5. Polyacrylate adsorption

Applying the two-layer model to the adsorption of polyacrylate onto a hematite coated ZnSe crystal implies that the adsorbed layer is much less than d_p, and that the effect of its refractive index can be ignored, or alternatively, that it has the same refractive index as the contacting solution. This is arguable for polymer absorption where loops and tails may protrude far in to the adsorbate solution.

The hydrodynamic diameters of PAA450K and PAA13M in solution at pH 2 and 13 (1 M NaCl) are ~350 and ~400 nm [5], which is of the order of the depth of penetration for ZnSe aqueous solution interfaces (Table 1). Thus, whilst the adsorbed segments of the polymer may constitute a negligibly thin layer, the unadsorbed segments will extend over a greater distance from the surface. The latter will probably behave more like the contacting solution as they will be solvated similarly. As it is not possible to determine the refractive index of adsorbed polyacrylate it has been assumed that the refractive index of all polymer segments is the same as that of a concentrated polymer solution.

The ZnSe/concentrated polymer solution interface characterisation is straight forward, because there is no complication associated with the presence of the hematite film, and is equivalent to the ZnSe/benzene calculations. A concentrated polymer solution, 1 wt.% of PAA450K made up at pH 13 in 1 M NaCl, was used, with the value of n_1 taken to be that of ZnSe (2.430 at 2125 cm^{-1}) and absorption values were recorded at 45° (A = 87.5 m^{-1}) and 50° (A = 63.7 m^{-1}) incident angles. The value for n_2 (the concentrated polymer solution) was found to be 1.360.

The result shows that the presence of polymer and electrolyte in the pH 13 solution medium increases the refractive index from that of water (1.320). While there is no direct literature data to compare this value to, measurements at a wavelength of 589 nm (16,978 cm^{-1}) show that 1 wt.% acetic acid has a refractive index of 1.33 and 1 M NaCl has a refractive index of 1.34 [16]. Both show a trend of increasing refractive index with increasing concentration in solution, therefore it would be expected that the above polymer solution would have a refractive index greater than that of water and that a result of n_2 = 1.360 is reasonable. This value has been used in all quantitation calculations.

On the assumption that the adsorbed polymer has equivalent optical properties to a concentrated polymer solution in contact with an uncoated ATR crystal, the refractive index of the porous hematite film adsorbed on ZnSe was found to be 2.417 (from the absorbances of a 50 ppm PAA13M solution of pH 13 and 1 M NaCl). The film porosity was found to be 32%, which is consistent to that found for the ZnSe–hematite/water system, i.e. again the refractive index of the electrolyte filling the pores influences the refractive index and the high molecular weight polymer used does not penetrate the film (as was also concluded from the adsorption of different molecular weight polyacrylates).

3.6. Adsorbed polymer quantification

Calculating adsorption densities from absorbances requires that ε, d_e and d_p are known. The latter were determined for polymer solutions as described above for the ZnSe/water system, whilst ε was determined from ATR measurements. Conventional transmission cell determination of ε could not be carried out because of the very small path-length cell required (<10 μm) and the viscosity of the polymer solutions. The results are summarised in Table 2. The slopes of the Beer's law calibrations are εd_e, which can be used directly in the two-layer adsorption density equation.

The adsorption isotherms obtained in this study were constructed by flowing polymer solutions of fixed concentrations past the cast hematite film consecutively. This strategy provides a consistent surface area for each known equilibrium

Table 2
Effective thickness (d_e) and depth of penetration (d_p) for 1 wt.% polymer (n_2 = 1.360) and ZnSe at pH 2 (n_1 = 2.426 at 1720 cm^{-1}) and pH 13 (n_1 = 2.424 at 1560 cm^{-1}), and polymer absorptivity (ε)

Adsorbing polymer and conditions	d_e (nm)	d_p (nm)	ε (m g^{-1})
PAA450K at pH 2	1419	894	1040
PAA450K at pH 13 (1 M NaCl)	1571	986	3600
PAA13M at pH 13 (1 M NaCl)	1571	986	1870

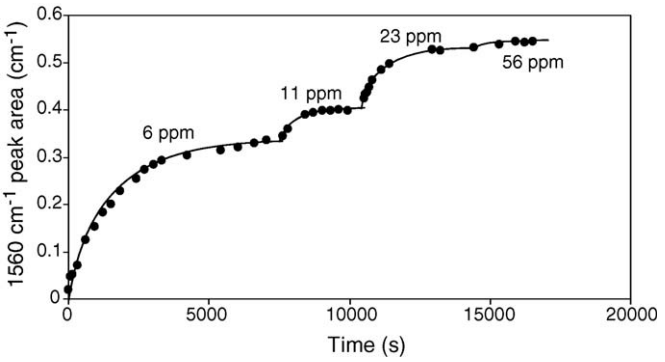

Fig. 3. Adsorption of PAA13M at pH 13 and 1 M NaCl (monitored by 1560 cm^{-1} peak area) at polymer concentrations of 6, 11, 23 and 56 ppm.

solution polymer concentration, as only one film is used and the solution concentration is maintained. A typical example is shown in Fig. 3. The adsorption data was found to fit the Langmuir isotherm model (Fig. 4), which enabled the pseudo equilibrium constants (K) and absorbances due to monolayer coverage (A_{max}) to be determined. The equilibrium constants are referred to as ''pseudo'' as the Langmuir model describes a true equilibrium but polymer adsorption is irreversible. A_{max} is used in conjunction with the previously determined values of ε, d_e and d_p to obtain monolayer surface densities.

The two-layer adsorption density equation is simply a restatement of Beer's law, in that it expresses the surface density in terms of a solution concentration that is equivalent to the surface coverage and the depth of the ATR measured layer (d_p), and is corrected for the solution species concentration, i.e.

$$\Gamma = [(A/\varepsilon d_e) - c_b]d_p$$

where $A/\varepsilon d_e$ is the equivalent solution concentration.

This assumes that adsorption occurs to a smooth flat surface and hence ignores surface roughness.

For a film consisting of 50–150 nm particles this is not valid, as adsorption could take place on both the ''hills'' and ''valleys'' formed. If the surface is treated as comprising monosized hemispheres the surface area is increased by a factor of 1.81 over that of a smooth surface. Furthermore, at pH 2 the mode of adsorption is bidentate chelation, as shown by the presence of both protonated and deprotonated carboxylate

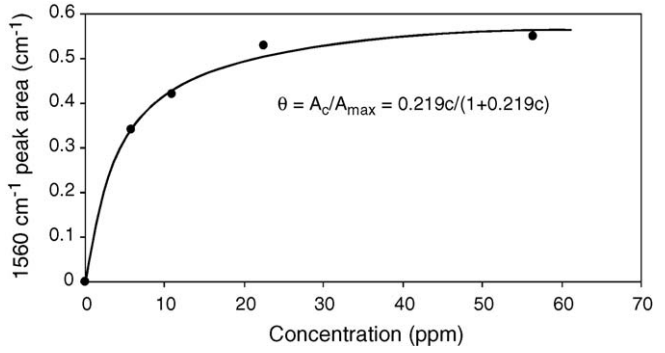

Fig. 4. Plateau absorbance values as a function of polymer concentration for PAA13M adsorption at pH 13 (1 M NaCl) and the subsequent Langmuir adsorption isotherm.

Table 3
Pseudo equilibrium constants (K), maximum integrated peak areas (A_{max}) and surface density (Γ) as determined from Langmuir isotherm fits and the two-layer adsorption model

Adsorbing polymer and conditions (peak)	K	A_{max} (m^{-1})	Γ (mg m^{-2})	
			Smooth	Rough
PAA450K at pH 2 (1720 cm^{-1})	0.236	76.3	57.5	31.7
PAA450K at pH 13 and 1 M NaCl (1560 cm^{-1})	0.481	76.5	13.3	7.3
PAA13M at pH 13 and 1 M NaCl (1560 cm^{-1})	0.219	60.9	20.5	11.3

stretches (Fig. 1, 1716 and 1543 cm^{-1}, respectively). The former is indicative of the loops and tails of the adsorbed polymer that protrude into the solution and the latter of the bound segments. Our previous work has shown that the unadsorbed:adsorbed segment ratio is 4:1 [4] and this has been allowed for in the calculations. At pH 13 (1 M NaCl) adsorption is by cation mediated van der Waals interactions, for which it is not possible to distinguish between adsorbed and unadsorbed segments, and the 1560 cm^{-1} carboxylate stretch is therefore a measure of the entire polyacrylate molecule [4]. The results are summarised in Table 3.

The adsorption densities obtained are much higher than typically reported for polymer adsorption, e.g. Lyklema reported values between 1.5 and 3 mg m^{-2} [5]. This is likely due to the different techniques used, i.e. adsorption on to particles in suspension as opposed to a film. Adsorbing polymer to particles in suspensions leads to flocculation of the particles by bridging. Once bridges are formed and flocculation occurs the surface available for further adsorption will be significantly reduced, and surface coverage is generally less than 20% [2,5–7].

The results reinforce the trains, loops and tails adsorption mechanism of polymers, as the measured surface densities are significantly greater than those calculated for adsorption of every carboxylate group of the polymer chain (i.e. an assembly of acrylate monomers). The maximum surface density (100% coverage) of an acrylate monolayer can be calculated from the unit area per monomer unit (0.154 nm^2, [6]) and is 0.776 and 1.01 mg m^{-2}, respectively, for polyacrylic acid (pH 2) and sodium polyacrylate (pH 13). This clearly indicates that the adsorption densities obtained are the equivalent of 7–40 of such layers and that hence the majority of the adsorbed polymer chain is in the loop and tail segments, with only a small fraction of the segments directly interacting with the surface (at most 2.5% and 11% for PAA450K at pH 2 and 13, and 6.5% for PAA13M at pH 13). The fractions bound at pH 13 found for PAA450K and PAA13M are what would be expected as a function of molecular weight, with the larger molecule having proportionally fewer bound segments. The larger molecules have a greater hydrodynamic diameter and hence a lower surface area to mass ratio, with proportionally less carboxylate groups being able to interact with the surface (unless significant uncoiling of the polymer occurs).

The surprising result is that for PAA450K at pH 2, where the bound fraction is 2.5% as opposed to the 20% found on the basis

of the intensities of the free and bound carboxylate groups [3], whose infrared absorptivities were assumed to be the same. If this is not the case then the values are not directly comparable. This problem does not arise with adsorption at pH 13 (1 M NaCl) as the solution and adsorbed carboxylates are indistinguishable, being the carboxylate ion associated with sodium ions.

4. Conclusions

The major uncertainties for quantifying adsorption densities on nano-particle films with ATR are the morphology (roughness) of the surface and the depth of penetration of the evanescent wave. The degree of roughness can only be an estimate and hence the adsorption densities, although consistent for similarly prepared surfaces, cannot be guaranteed to be correct in an absolute sense. The uncertainty associated with the depth of penetration of the infrared radiation affects the results obtained similarly. For this to be determined accurately detailed knowledge of the optical properties of the interface is required, i.e. the refractive indices of all components of the solution/substrate/adsorbate interface and the polarisation fraction of the radiation. The solution equivalent concentrations derived from the application of Beer's law calibrations in solution are directly used in the adsorption density equation and thus assume that the infrared adsorptivities of the free and adsorbed molecules or segments are the same. There is no guarantee of this. Despite these limitations, our results indicate that surface densities obtained for adsorption on nano-particle films deposited on an ATR element are realistic in an absolute sense and accurate in a relative sense.

From this study it is clear that at pH 13 higher molecular weight polymers adsorb to hematite with a higher fraction of loops and tails than do lower molecular weight polyacrylates. For the same polyacrylate, the adsorption at pH 2 is much greater than at pH 13. This may well be a function of the different coiling of the polymer at different pH and the adsorption mode changing from bi-dentate chelation at pH 2 to van der Waals attraction at pH 13 (1 M NaCl), which facilitates the adsorption of polyacrylate to the hematite surface through the presence of sodium ions [3,4].

Acknowledgements

This research has been supported by the Australian Government's Cooperative Research Centre (CRC) Program, through the Parker CRC for Integrated Hydrometallurgy Solutions. This support is gratefully acknowledged. L.J.K. is grateful for the support of an Australian Research Council Postgraduate Award.

References

[1] L.J. Connolly, D.O. Owen, P.F. Richardson, Light Met. (1986) 247–261.
[2] F. Jones, J.B. Farrow, W. van Bronswijk, Colloid Surf. A: Physicochem. Eng. Aspects 135 (1998) 183.
[3] L.J. Kirwan, P.D. Fawell, W. van Bronswijk, Langmuir 19 (2003) 5802.
[4] L.J. Kirwan, P.D. Fawell, W. van Bronswijk, Langmuir 20 (2004) 4093.
[5] J. Lyklema, Flocculation and Dewatering, Engineering Foundation, New York, 1989, pp. 1–20.
[6] D.N. Misra, J. Colloid Interf. Sci. 181 (1996) 289.
[7] F.R. Eirich, J. Colloid Interf. Sci. 58 (1977) 423.
[8] R.P. Sperline, S. Muralidharan, H. Freiser, Langmuir 3 (1987) 198.
[9] R.P. Sperline, Y. Song, H. Freiser, Langmuir 8 (1992) 2183.
[10] R.P. Sperline, H. Freiser, Langmuir 6 (1990) 344.
[11] N.J. Harrick, Infrared Reflection Spectroscopy, Harrick Scientific Corporation, New York, 1987.
[12] A. Feldman, D. Horowitz, R. Waxler, M. Dodge, National Bureau of Standards (US) Technical Note #993, 1979.
[13] L.D. Tickanen, M.I. Tejedor-Tejedor, M.A. Anderson, Appl. Spec. 46 (1992) 1848.
[14] T.G. Goplen, D.G. Cameron, R.N. Jones, Appl. Spec. 34 (1980) 657.
[15] P.W. Atkins, Physical Chemistry, Oxford University Press, Oxford, 1988.
[16] D.R. Lide (Ed.), CRC Handbook of Chemistry and Physics, 86th ed., CRC Press, Boca Raton, 2004.